Mon. Not. R. Astron. Soc. **288,** 1004–1014 (1997)

DB white dwarf evolution in the frame of the full spectrum turbulence theory

O. G. Benvenuto★† and L. G. Althaus★‡

Facultad de Ciencias Astronómicas y Geofísicas, Universidad Nacional de La Plata, Paseo del Bosque S/N, (1900) La Plata, Argentina

Accepted 1997 March 5. Received 1997 February 27; in original form 1997 January 6

ABSTRACT

We present an analysis of the evolution of carbon–oxygen DB white dwarfs (helium-rich envelope) for a wide range of effective temperatures and luminosities. To this end, we employ a full stellar evolution code, in which we include a new equation of state for helium plasmas recently developed by Saumon, Chabrier & Van Horn and new OPAL radiative opacities. The most important feature of our models is that the transport of energy by convection is described by the full spectrum turbulence theory. In particular, we have adopted two versions of this theory for stellar convection: the Canuto & Mazzitelli theory and the more recent, self-consistent theory developed by Canuto, Goldman & Mazzitelli. Both theories, which have no free parameters and account for the whole spectrum of turbulent eddies, represent a great improvement compared to the mixing-length theory approach used thus far in almost all white dwarf studies. Neutrino energy losses as well as crystallization were taken into account. In order to explore the sensitivity of our results to various input model parameters, we vary the model mass from 0.5 to 1.0 $M_{\odot}$ in intervals of 0.1 $M_{\odot}$, and the helium layer mass in the interval of $10^{-6} \leq M_{\rm He}/M_{*} \leq 10^{-2}$.

The emphasis is put mainly on the behaviour of the evolving outer convection zone. In particular, we analyse the dependence of the location of the theoretical blue edge of the instability strip on the various input parameters. We find that the new ingredients we have incorporated in this study – mostly the new formulations for stellar convection – lead to theoretical blue edges in agreement with observations of pulsating DB white dwarfs. In this context, the Canuto, Goldman & Mazzitelli self-consistent theory yields theoretical blue edges somewhat hotter than those given by the Canuto & Mazzitelli theory, which is more consistent with a recent determination of the effective temperature of the hot DBV GD 358. Contrary to previous results, we find that, according to the new theories for convection, non-variable DB white dwarfs falling within the instability strip cannot be low-mass configurations.

In order to compare with previous computations, we include in our calculations the most common parametrizations of the mixing-length theory usually employed in almost all previous white dwarf studies. In this context, we find that the ML2 parametrization provides a reasonable agreement with the observed blue edge for the DB instability strip. However, the profile of the outer convective zone given by the mixing-length theory is markedly different from that given by both of the new convective formulations.

Key words: convection – stars: evolution – stars: variables: other – white dwarfs.

★E-mail: obenvenuto@fcaglp.fcaglp.unlp.edu.ar (OGB); althaus@fcaglp.fcaglp.unlp.edu.ar (LGA)
†Member of the Carrera del Investigador Científico, Comisión de Investigaciones Científicas de la Provincia de Buenos Aires (CIC), Argentina.
‡Fellow of the Consejo Nacional de Investigaciones Científicas y Técnicas (CONICET), Argentina.

1 INTRODUCTION

White dwarf (WD) is the most common fate for stars. It is known that approximately 90 per cent of stars evolve to this state. Since the pioneering work of Chandrasekhar (1939), the structure of these objects is very well understood, and their evolution, which can be treated in first approximation as a simple cooling problem (Mestel 1952), is simpler than that of the nuclear-burning stars (for an introduction see, e.g., Shapiro & Teukolsky 1983 and Koester & Chanmugam 1990; for a review see D'Antona & Mazzitelli 1990). Since fast computers became available, WD evolution has been computed by means of full stellar evolutionary codes and with an increasing degree of sophistication, particularly in the treatment of the non-degenerate layers, which enabled the construction of very detailed models. From then on, WD evolution has been the subject of many papers such as, e.g., Lamb & Van Horn (1975); Iben & Tutukov (1984); Koester & Schönberner (1986); D'Antona & Mazzitelli (1989); Tassoul, Fontaine & Winget (1990); Wood (1992); Benvenuto & Althaus (1995); Althaus & Benvenuto (1996, 1997a, b) and Oswalt et al. (1996) among others.

The interest in cool WDs has greatly increased since the existence of pulsations in some of them was established. Pulsating WDs, which are restricted to narrow instability strips, represent a powerful tool for providing a view on the innermost structure of these stars that would be otherwise inaccessible. In particular, the boundaries of the instability strips give us the possibility of probing the thermal structure of the outer convection zone (OCZ) of WDs where pulsation driving occurs. In this context, numerous studies in the past have revealed that the determination of the position of the theoretical hot (blue) edge of instability strips in the Hertzsprung–Russell (HR) diagram is mostly sensitive to the treatment of convection. Moreover, a match to the observed location of the blue edge would yield a way of constraining the convective efficiency assumed in theoretical models (see, e.g., Winget et al. 1982, 1983; Tassoul et al. 1990; Wesemael et al. 1991; Bradley & Winget 1994; and Bradley 1996 and references therein).

The aforementioned studies treat the energy transport by convection in the frame of the mixing-length theory (MLT) (Böhm-Vitense 1958), which is undoubtedly one of the weakest points in the theoretical description of the models. Among other crude approximations, the MLT assumes the spectrum of turbulent eddies to be represented by one large eddy. Worse still, certain free parameters appearing in the description of the model are not predicted by the theory. Needless to say, the existence of such free parameters weakens the predictive power of the MLT (see Section 3.3 for more details).

Fortunately, there has been in recent years a renewed effort to formulate new theories of convection. In particular, Canuto & Mazzitelli (1991, 1992, hereafter CM) and, more recently, Canuto, Goldman & Mazzitelli (1996, hereafter CGM; see also Canuto 1996) developed two theories based on a fundamentally different approach from that of the MLT. They considered turbulent convection as being described not by one, single-size eddy but by a whole spectrum of eddies. Because of this, such theories may be called full spectrum turbulence theories (FST).

The CM theory (CM) has been employed to study different kinds of problems (see, e.g., D'Antona, Mazzitelli & Gratton 1992, Paternó et al. 1993, D'Antona & Mazzitelli 1994, Stothers & Chin 1995 and also Canuto 1996 for further references). Recently, Althaus & Benvenuto (1996) applied the CM to the study of the evolution of pulsating DB WDs for different stellar masses and metallicities. They found that the effective temperature $T_{\rm eff}$ of the DB blue edge of the instability strip determined by Thejll, Vennes & Shipman (1991) is nicely accounted for by the CM. Mazzitelli & D'Antona (1991) also applied the CM to a 0.55-$M_{\odot}$ DB WD, and find for the $T_{\rm eff}$ of the blue edge a value consistent with observations. More recently, Althaus & Benvenuto (1997a, hereafter AB97) employed the CM in the computation of the evolution of low- and intermediate-mass helium WDs.

Much more recently, CGM developed a self-consistent theory (CGM) to treat stellar convection; this represents an improvement compared to CM, for it considers a self-consistent rate of energy input. At low and intermediate convective efficiencies, CGM provides higher convective fluxes than CM. CGM applied the new theory to compute the evolution of a solar model, finding results quite similar to those given by CM. However, the extent of the overshooting required to fit the solar radius is substantially smaller than in the CM case, which is in better agreement with recent observational data. Also, the age of the globular cluster M68 is reduced by ≈ 1 Gyr with respect to CM. It is worth mentioning that for these objects, the evolutionary results obtained with either CM or CGM do not differ appreciably. Thus, based on these calculations, it seems difficult to discriminate between them. However, fortunately, as we shall detail below (see Section 4), DB WDs give a clear indication that (at least in the realm of WDs) the CGM matches the observations much better than the CM.

In this paper we carry out a detailed analysis of the evolution of carbon–oxygen DB WDs in the range of intermediate $T_{\rm eff}$. To this end, we employ a full stellar evolution code in which we include a physical description as updated and detailed as possible, such as a new equation of state (EOS) for helium composition, new OPAL radiative opacities and, as mentioned, the CM and CGM models. In particular, we focus our attention on the study of behaviour of the evolving OCZ both in the frame of the FST and in that of the MLT. Short accounts of the main results of this study can be found in Althaus & Benvenuto (1996, 1997b).

Apart from pulsational studies, there are other strong motivations for constructing improved evolutionary sequences of WDs. One is the already classical study of the age of the Galactic disc by means of the WD luminosity function (e.g. Wood 1992; Oswalt et al. 1996). Another is that, thanks to the *Hubble Space Telescope*, it has been possible to detect the low-luminosity tail of the WD population in open and globular clusters. Thus, employing WD evolutionary tracks, it is possible to measure the age and distance of such clusters in an independent way (see, e.g., Richer et al. 1995, Von Hippel, Gilmore & Jones 1995 and Renzini et al. 1996).

In order to explore the sensitiveness of our results to various input model parameters, we vary the model mass, the metal abundance and the thickness of the helium layer. We present DB WD models with masses ranging from 0.5 to 1.0 $M_{\odot}$ at intervals of 0.1 $M_{\odot}$ (which covers the observed

mass range of isolated carbon–oxygen WDs; see Bergeron, Saffer & Liebert 1992 and Bragaglia, Renzini & Bergeron 1995), and we use $10^{-6}M_* \leq M_{\rm He} \leq 10^{-2}M_*$ for the helium layer mass. Neutrino energy losses and crystallization are also taken into account.

The remainder of this paper is organized as follows. We begin in Section 2 by giving a description of our evolutionary code and the procedure adopted for constructing the initial models. In Section 3 we comment on the main physical ingredients that we included in this study; Section 4 is devoted to the analysis of the results, and in Section 5 we summarize our findings.

2 NUMERICAL CODE AND INITIAL MODELS

The calculations were performed with the same evolutionary code that we employed in our previous works on WD evolution. Its architecture is based on the work of Kippenhahn, Weigert & Hofmeister (1967). We have made only slight changes to the code employed in AB97. In particular, we improved the atmospheric integration method. We assumed a grey model with a temperature distribution $T(\tau)$ such that the flux constancy is satisfied at each optical depth τ. To this end, we adopted for $T(\tau)$ the following relation:

$$T^4(\tau) = 0.75T_{\rm eff}^4[\tau + q(\tau)], \tag{1}$$

with

$$q(x) = 17/24 + E_4(x) - E_2(x)/3 + E_3(x)/2 - 1.5E_5(x), \tag{2}$$

where $E_n(x)$ is the exponential integral of order n (see Mihalas 1970 for details).

It has been known for quite some time that carbon–oxygen WDs undergo crystallization (see Van Horn 1968). We have included this phenomenon in our computations in the same way as in Benvenuto & Althaus (1995). In particular, to include the release of latent heat during the propagation of the crystallization front, we write the energy conservation equation as

$$\frac{\partial l}{\partial m} = -\varepsilon_\nu - T\frac{\partial S}{\partial t} + \frac{\partial q_l}{\partial m}\dot{m}, \tag{3}$$

where S is the entropy per gram, $\dot{m}$ represents the velocity of propagation of the crystallization front in the Lagrangian coordinate, and q_l is the latent heat per gram. The second term is the gravitational potential energy, in which both thermal and compression contribution are present, while the third term measures the rate at which latent heat is released. The term ε_ν represents the neutrino energy losses (see Section 3.2). Latent heat was distributed over a small mass interval, and the location of the crystallization front as well as the released latent heat were calculated at each iteration.

To overcome numerical difficulties of convergence arising from the inclusion of the latent heat and, more importantly, from the non-local nature of the FST, we found it necessary to divide our models in about 2000 mesh points. For further details concerning the modifications carried out in our numerical code to cope with such difficulties, we refer the reader to AB97.

The initial models were obtained following the procedure described in AB97. The core chemical composition profile of these models (see fig. 1 of Benvenuto & Althaus 1995) was computed by D'Antona & Mazzitelli (1989) for a 0.55-$M_\odot$ WD model. We mention that we have not included changes in the interior composition for models of different masses, despite the fact that these changes should indeed exist because of the differences in the pre-WD evolution of progenitor objects. Since the actual value of the thickness of the outer helium layer is still an open question (see Tassoul et al. 1990 and Bradley & Winget 1994), we allow the helium layer mass to vary in the range $10^{-6}M_* \leq M_{\rm He} \leq 10^{-2}M_*$. We have not taken into account models with thinner helium layers because, at $T_{\rm eff} \gtrsim 15\,000$ K, convective mixing would eventually turn such models into objects with carbon-dominated outer layers (see also Tassoul et al. 1990). Such objects have never been detected (D'Antona & Mazzitelli 1990). Finally, the He/C–O transition zone was assumed to be discontinuous.

3 INPUT PHYSICS

3.1 Equation of state

In this study, we have considered three different EOSs. As WDs gradually cool, the Saha equation becomes progressively inadequate to describe the ionization balance in the outer layers. Instead, covolume, van der Waals, Coulomb and degeneracy among others effects must be taken into account in order to achieve a sufficiently detailed thermodynamic treatment. For such purpose, we have adopted the recent EOS developed by Saumon, Chabrier & Van Horn (1995). This EOS, calculated by means of the free energy minimization technique, describes the thermodynamics of hydrogen- and helium-rich plasmas, and was specially devised for treating the structure of low-mass stars and giant planets. This EOS is the most detailed treatment of such plasmas presently available.

We adopted the Saumon et al. (1995) EOS for helium composition in the range of pressure and temperature limited by $\log P({\rm dyn\ cm^{-2}}) < 19$ and by $\log T({\rm K}) < 7$. Outside these limits (or for carbon composition) and up to a density of $\rho = 2 \times 10^3$ g cm^{-3} we employed an updated version (Mazzitelli 1993, private communication) of the EOS of Magni & Mazzitelli (1979). Finally, for higher densities, we developed a detailed EOS based on the results for the one-component plasma with a uniform background of electrons. Such treatment has been presented before, and we refer the reader to Benvenuto & Althaus (1995) and AB97.

3.2 Opacities and neutrino emission

Conductive opacities were taken from the works of Itoh and collaborators and Hubbard & Lampe (1969). These opacities include the full contributions relevant to the WD domain.

Radiative opacities for hydrogen-free composition at $T \gtrsim 7000$ K were taken from the OPAL data library kindly provided to us by F. Rogers (1994, private communication). For lower temperatures, we had to rely on other sources, in particular the tabulation of Cox & Stewart (1970) which,

albeit rather old, matches acceptably well the OPAL data at those low-temperature conditions in which both values exist. To test the sensitivity of the location of the theoretical blue edge to the metallicity Z, we considered two values: $Z=0$ and 10^{-3}.

As stated earlier, we have included different mechanisms of neutrino emission relevant to hot WD stars. Photo-, plasma- and bremsstrahlung neutrino were taken from the works of Itoh and collaborators. For more details on these topics, see AB97, and references therein.

3.3 Convection

In our calculations we have considered two kinds of treatment for convection: the MLT and the CM and CGM.

The MLT is the standard method of dealing with convection in stellar evolution calculations. The fact that the MLT is a simple model able to provide a reasonable description of turbulent convection in stars and, more importantly, that it can be easily implemented in evolutionary codes, has undoubtedly contributed to its popularity since its formulation for stellar studies by Böhm-Vitense (1958). However, the MLT is a crude description of stellar turbulent convection. For instance, the one-eddy approximation is inadequate to describe the almost inviscid stellar interiors. Another limitation is that it contains free parameters not predicted by the theory. In particular, in the Böhm-Vitense formulation, the MLT involves three length-scales which, in most stellar applications, are reduced to a single one, chosen to be some multiple of the pressure scaleheight H_P: $l=\alpha H_P$ where l, the mixing length, is the average distance travelled by the eddies before releasing their energy excess in the surrounding medium, and α is a free parameter; α, usually derived from solar radius adjustments, is generally larger than unity, in contrast with the basic postulates of the MLT. Obviously, the solar convective envelope is in thermodynamic conditions vastly different from the ones present in WDs, thus making the use of the solar α in the WD envelopes highly suspicious. Another fitting method is to adjust the value of α from observations of pulsating WDs. The same α is applied then to the rest of the WD evolution and, even worse, to the whole OCZ. In this context, recent hydrodynamical calculations in ZZ Ceti variables (with hydrogen-rich outer layers, i.e., DAV WDs; Ludwig, Jordan & Steffen 1994) reveal that the temperature stratification throughout the OCZ cannot be reproduced with models obtained within the MLT formalism with a *single* value of α.

CM have quantitatively shown that the one-eddy approximation is inadequate, and have developed a treatment in which the convective flux is contributed by a wide *spectrum* of eddy sizes. Such spectrum is computed on the basis of detailed theories of turbulence rather than postulated to be a δ-function as in the MLT case. In this way, these authors avoid dealing with free parameters in their description of convection. CM fit their theoretical results for the convective flux F_c with the following expression:

$$F_c=KTH_p^{-1}(\nabla_{conv}-\nabla_{ad})\Phi, \tag{4}$$

where $K=4acT^3/3\kappa\rho$ is the radiative conductivity, ∇_{conv} and ∇_{ad} are, respectively, the convective and adiabatic temperature gradients, and Φ is given by

$$\Phi=\left(\frac{K_0}{1.5}\right)^3 a_1\Sigma^m[(1+a_2\Sigma)^n-1]^p. \tag{5}$$

Here K_0 is the Kolmogorov constant (assumed to be 1.8), and the coefficients are given by $a_1=24.868$, $a_2=9.7666\times10^{-2}$, $m=0.14972$, $n=0.18931$, and $p=1.8503$; Σ, a measure of the convective efficiency, is defined as $\Sigma\equiv4A^2(\nabla_{conv}-\nabla_{ad})$. For comparison, in the standard MLT of Böhm-Vitense (1958), the parameters of equation (5) have the values $a_1=9/8$, $a_2=1$, $m=-1$, $n=1/2$, and $p=3$. Finally, A is given by

$$A=\frac{c_p\rho^2\kappa z^2}{12acT^3}\left(\frac{g\delta}{2H_p}\right)^{1/2}, \tag{6}$$

where z is the mixing length (*not* to be confused with the mixing length of MLT; see below), and the other quantities have their usual meaning (see CM for further details). ∇_{conv} is given by

$$\nabla_{conv}=\frac{(\nabla_r+\Phi\nabla_{ad})}{1+\Phi}, \tag{7}$$

where ∇_r is the radiative gradient.

Recently, CGM proposed a self-consistent FST to calculate stellar convection based on a simplified treatment of the non-linear interactions among the eddies. The CGM model differs from CM in that the energy input from the source (buoyancy) into the turbulence depends now on both the source and turbulence itself. This feature represents an improvement with respect to CM and makes CGM a self-consistent theory.

In terms of S, the dimensionless product of the Rayleigh and Prandtl numbers, CGM fit their theoretical results with the expression

$$\Phi=F_1(S)F_2(S), \tag{8}$$

where

$$F_1(S)=\left(\frac{K_0}{1.5}\right)^3 aS^k[(1+bS)^l-1]^q. \tag{9}$$

Here $S=40.5\Sigma$ and the coefficients are given by $a=10.8654$, $b=4.89073\times10^{-3}$, $k=0.149888$, $l=0.189238$, and $q=1.85011$, and

$$F_2(S)=1+\frac{cS^{0.72}}{1+dS^{0.92}}+\frac{eS^{1.2}}{1+fS^{1.5}}, \tag{10}$$

where $c=1.08071\times10^{-2}$, $d=3.01208\times10^{-3}$, $e=3.34441\times10^{-4}$, and $f=1.25\times10^{-4}$.

For low and intermediate S values, CGM predict convective fluxes higher (up to a factor of 3) than CM. In particular, the flux ratio is maximal at $\log S\approx2.5$. This difference in the values of the convective flux is due exclusively to the self-consistent nature of the CGM model (see CGM for details). By contrast, at high S values both theories yield similar results. Comparing with MLT predictions, both of the FST treatments provide larger (smaller) convective flux at high (low) convective efficiency.

A key improvement of the FST is the absence of free parameters. In fact, the mixing length is taken as $l=z$, where

z is the distance from the top of the convection zone to the point where V_{conv} is computed. This accounts for the vertical stacking of eddies, and nicely fits the observed solar radius. This choice for the mixing length makes this class of theories essentially non-local, which makes them more difficult to treat adequately in evolutionary computations (see Section 2).

In order to compare with previous results, we have included in our calculations the most usual parametrizations of the MLT employed in most of WD calculations. These versions are associated with different convective efficiency and differ among them in the choice of the coefficients appearing in the expressions of the convective flux, the average velocity of convective elements, and the convective efficiency. Specifically, we have restricted ourselves to the three parametrizations discussed in Tassoul et al. (1990): the ML1 version of MLT, which corresponds to the standard treatment of Böhm-Vitense with $\alpha=1$, the ML2 version due to Böhm & Cassinelli (1971) with $\alpha=1$ (this version decreases the horizontal energy-loss rate and therefore increases the convective efficiency compared to the ML1) and, finally, the ML3 version, which is the same as the ML2, but with $\alpha=2$ and thus with a greater convective efficiency than that of the ML2 version.

4 EVOLUTIONARY RESULTS

We now summarize the main results of our calculations. We have computed the evolution of DB WDs with masses of $M/M_{\odot}=0.4, 0.5, 0.6, 0.7, 0.8, 0.9$ and 1.0; for three helium layer thickness $\log q_{He}=-2$, -4 and -6; and for two metallicities: $Z=10^{-3}$ and 0.0. Each of these sequences were evolved from the hot WD stage down to $\log L/L_{\odot}\lesssim -5$.

In Fig. 1 we show the HR diagram for DB WD models with $Z=10^{-3}$ and $\log q_{He}=-2$ with the CGM model. Models constructed with these assumptions will be hereafter considered as the reference ones and, unless some difference is explicitly stated, we shall refer to them. For the evolutionary stages shown here, the HR diagram is fairly insensitive to the choice of the exact values of Z and $\log q_{He}$, and to the theory of convection. The evolutionary tracks are nearly straight lines, as expected for such strongly degenerate configurations. We have chosen to start our computations with models as bright as possible, a point which is limited by our method for constructing the initial models. In all cases, we have been able to start the computations from initial models characterized by T_{eff} values much higher than the T_{eff} of the observed blue edge of the DB instability strip (defined by the two vertical solid lines in the Fig. 1).

The neutrino luminosity of the models in the high-T_{eff} domain is depicted in Fig. 2. As is well known, neutrino emission is the main cooling process during these phases of WD evolution, lowering the core temperature substantially. We find that even at those T_{eff} characteristic of the DB instability strip, neutrino losses are *not* negligible and should be fully taken into account. Particularly for lower mass models, neutrino emission is at least as effective as photon emission in releasing the stellar energy content *even* for models inside the DB instability strip.

In Fig. 3 we show the surface gravity versus T_{eff} for DB WD models of $M/M_{\odot}=0.5$, 0.6 and 0.7. It is clearly noticeable that the effects of finite temperature are not negligible

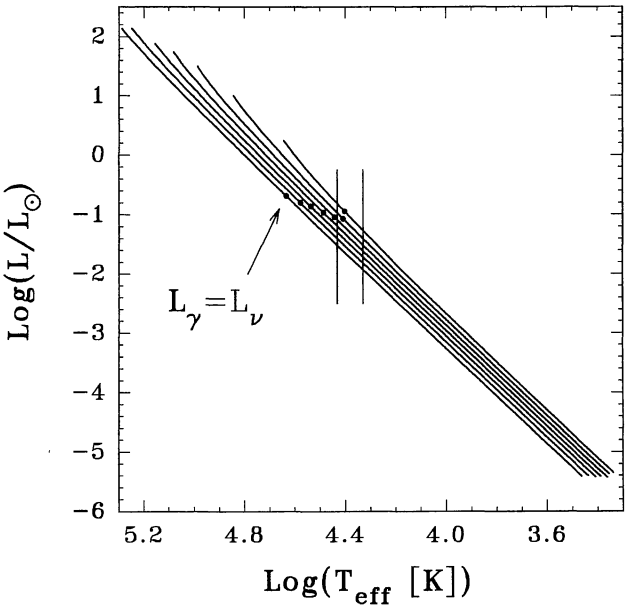

Figure 1. The Hertzsprung–Russell diagram for WD DB models with $Z=10^{-3}$ and $\log q_{He}=-2$ according to the CGM model of convection (the reference model set). From right to left, tracks corresponding to models with $M/M_{\odot}$ from 0.4 to 1.0 in steps of 0.1 are depicted. For each model we also show the locus for which the neutrino luminosity equals photon luminosity ($L_{\nu}=L_{\gamma}$). Vertical lines indicate the position of the DB instability strip. Note that for the lowest masses considered here, neutrino losses are not negligible during the pulsation stage.

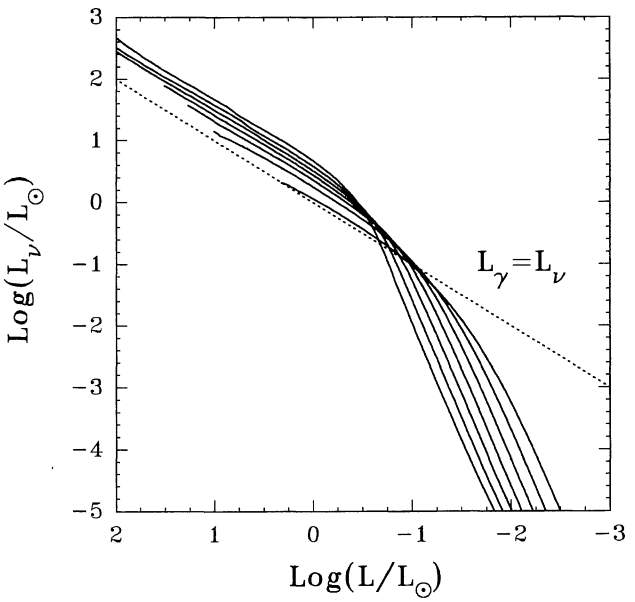

Figure 2. Neutrino luminosity versus photon luminosity for the reference models. For low neutrino luminosities, the curves correspond, from left to right, to models with masses from $M/M_{\odot}=1.0$ to 0.4 in steps of -0.1. For the sake of reference, the line $L_{\gamma}=L_{\nu}$ is also shown.

(see also Koester & Schönberner 1986 for similar results). For example, a cool 0.5-$M_{\odot}$ model has a surface gravity comparable to that of a hot 0.6-$M_{\odot}$ model. This result is independent of the adopted treatment of convection and of the value of the metallicity.

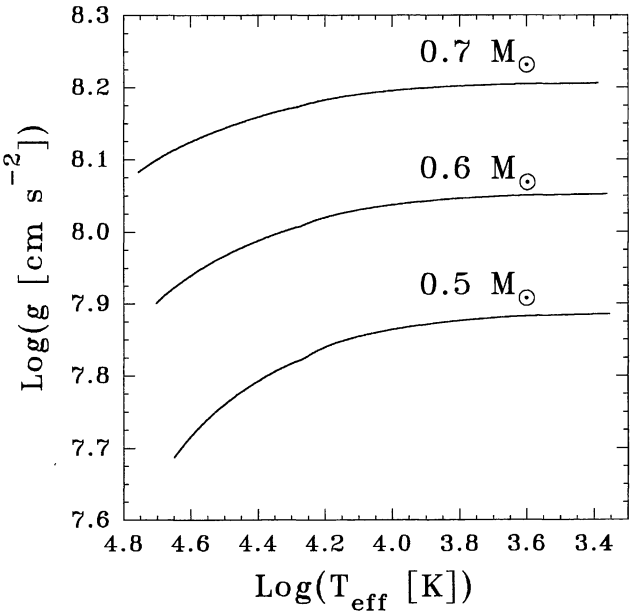

Figure 3. The surface gravity versus $T_{\rm eff}$ for the reference models. Note the importance of thermal effects even in rather massive models.

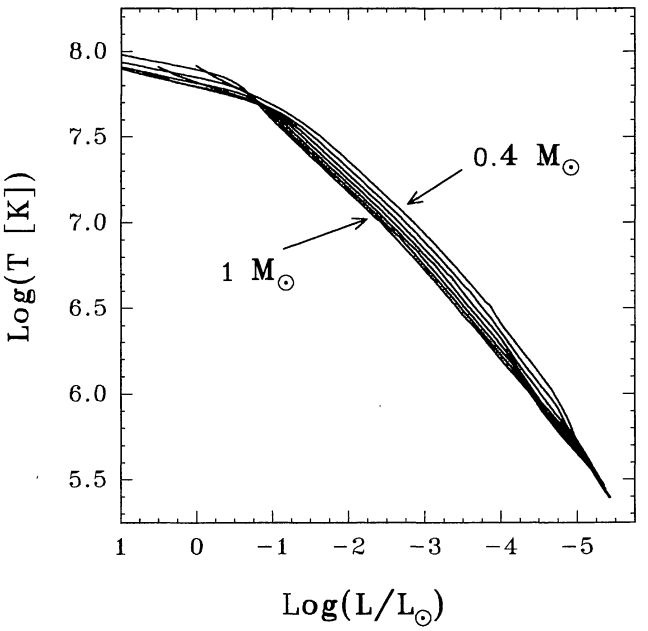

Figure 4. The behaviour of the central temperature as a function of photon luminosity for the reference models.

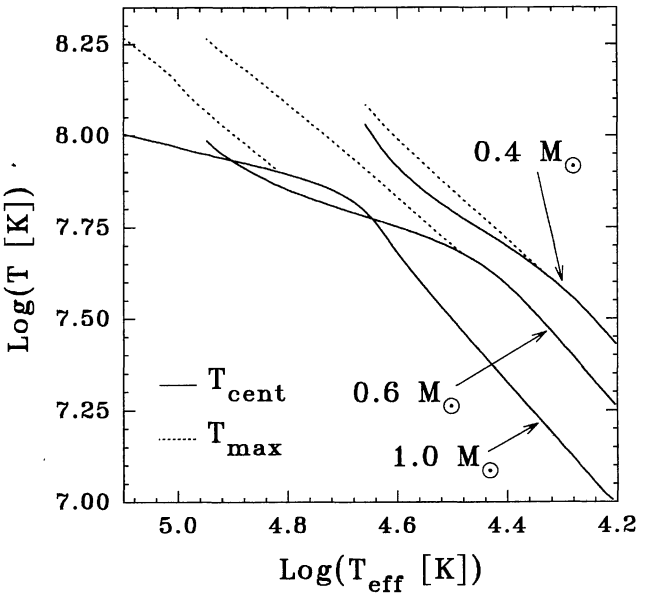

Figure 5. The central and maximum temperatures versus $T_{\rm eff}$ for the hot stages of DB WD reference models of $M/{\rm M}_{\odot}=0.4$, 0.6 and 1.0. At high $T_{\rm eff}$, neutrino losses lead to maximum temperatures appreciably different from the central temperature. This effect is more noticeable for the more massive models. For lower $T_{\rm eff}$, the maximum temperature occurs at the centre of the object.

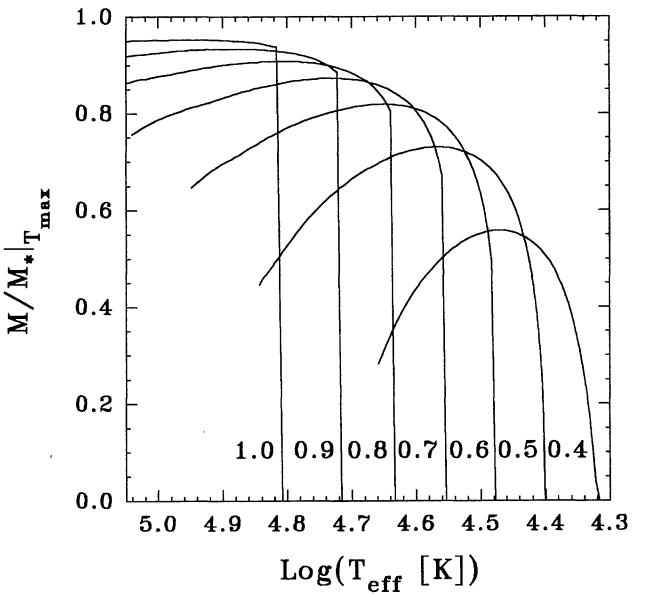

Figure 6. The location of the maximum temperature in the Lagrangian coordinate versus $T_{\rm eff}$ for the reference models. For the more massive models the position of the maximum temperature suddenly falls down from the outer layers to the centre. During this stage, $M/M_*|_{T_{\rm max}}$ is an almost discontinuous function of $T_{\rm eff}$.

In Fig. 4 we depict the behaviour of the central temperature as a function of the photon luminosity for the reference models throughout their entire evolution. Fig. 5 describes the central and maximum temperatures versus $T_{\rm eff}$ for the hot stages of the reference models of $M/{\rm M}_{\odot}=0.4$, 0.6 and 1.0. As stated above, at high luminosities, neutrino losses are so strong that they lead to maximum temperatures appreciably different from the central ones. This effect is especially noticeable for the more massive models, but for such objects neutrino losses become irrelevant at higher luminosities compared to less massive models. For lower $T_{\rm eff}$ values, the maximum temperature occurs at the centre of the object.

The location of the maximum temperature in the Lagrangian coordinate as a function of the $T_{\rm eff}$ for the reference models (see Fig. 6) is worthy of comment. Note that for the

more massive models, the position of the maximum temperature suddenly drops from the outer layers to the centre. During this stage, the WD interior is almost isothermal, and hence a slight change in the temperature profile causes $M/M_*|_{T_{max}}$ to be an almost discontinuous function of T_{eff}.

In the range of luminosities considered here, the models develop a crystalline core as a result of Coulomb interactions between ionized nuclei (see, e.g., Van Horn 1968 and Benvenuto & Althaus 1995). The onset of crystallization at the centre of our models with masses of $M/M_\odot = 0.4$, 0.5, 0.6, 0.7, 0.8, 0.9 and 1.0 occurs at $\log L/L_\odot = -3.84$, -3.56, -3.32, -3.10, -2.88, -2.65 and -2.40, respectively. The process of growth of the crystal phase is fairly similar to that given in Benvenuto & Althaus (1995) and will not be repeated here.

The photon luminosity versus the age for the reference models is shown in Fig. 7. We assumed the zero age to correspond to the first model we considered after the artificial heating procedure was completed. We stress that the age values of our models are strongly dependent upon our choice of zero-age point. Thus, if we want to determine precisely the age of WD during hot stages, we must add the time spent by the objects in the pre-WD evolution.

The effects of changing the thickness of the helium outer layer on the evolution of cool WD models has been amply discussed in the literature and will not be repeated here (see, e.g., Tassoul et al. 1990 and Wood 1992).

The dimensionless convective temperature gradient as a function of the pressure throughout the entire convective zone is shown in Fig. 8. The results correspond to the 0.6-$M_\odot$ DB WD model with $T_{eff} = 26\,400$ K and $Z = 10^{-3}$ according to CGM and CM, and to the ML2 and ML3 versions of the MLT. The higher convective fluxes characterizing CGM yield slightly deeper convective zones than those given by CM. Note the presence of a narrow peak in ∇_{conv} at $P \approx 10^7$ erg cm^{-3}, which corresponds to conditions of very inefficient convection. In such conditions, the ordering at increasing efficiency (decreasing ∇_{conv}) is CM, CGM, ML2 and ML3. However, at higher pressures (i.e., at deeper layers) the sequence of efficiencies is CM, ML2, CGM and ML3. This behaviour is essential in fixing the thermal structure of the envelope and, consequently, the size of the OCZ and the pulsational properties of the models.

The thermal profile of the envelopes of the same object according to the different treatments of convection is shown in Fig. 9. Note that at $\log q \approx -14.8$, which corresponds to $P \approx 10^7$ erg cm^{-3}, there is no peak, so the general trend of the thermal profile is dominated by the behaviour of ∇_{conv} at deeper layers, where convective efficiency is higher. It is clear that above and below the OCZ the values of the temperatures are independent of the treatment of convection. Except for the outermost layers near the peak of ∇_{conv}, we note that at a given value of $\log q$, at increasing temperature, the ordering of the treatments is ML3, CGM, ML2 and CM, i.e., just the opposite of the convective efficiency quoted above.

The evolution of the size of the OCZ as a function of T_{eff} for the 0.4-$M_\odot$ DB WD according to different theories of convection is depicted in Fig. 10. In this case we have chosen $\log q_{He} = -2$ and two values of Z, namely $Z = 10^{-3}$ and 0.0. It is clear from this figure that the profile of the OCZ predicted both by CM and CGM is qualitatively different from that predicted by any version of the MLT (see also Althaus & Benvenuto 1996). In the case of ML1, ML2 and ML3, the results are similar to those presented by Tassoul et al. (1990). Note that in the case of CM and CGM, the growth of the OCZ takes place in two rather abrupt steps, while in the MLT it is smoother. Note, also, that for very hot or very cool objects the OCZ size does not depend upon the

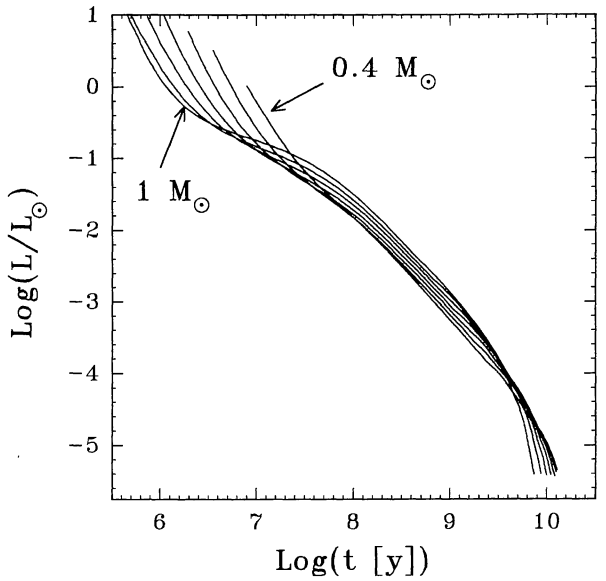

Figure 7. The photon luminosity versus the age for the reference models. These results do not depend on the treatment of convection. For the definition of the time origin see text.

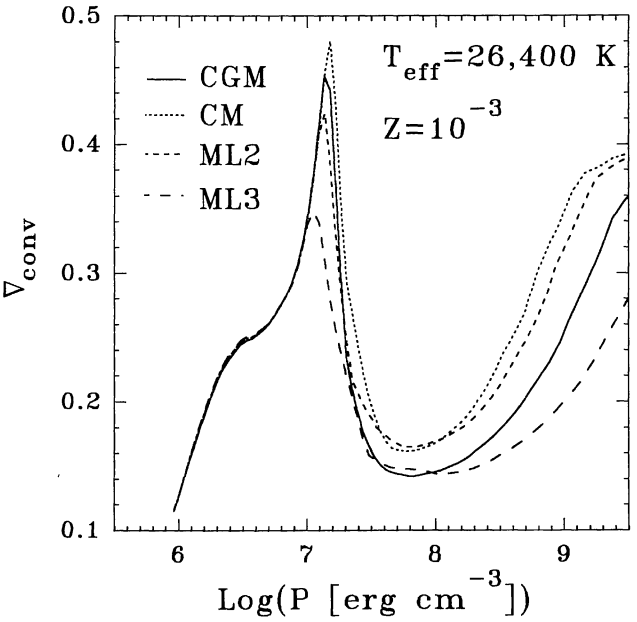

Figure 8. The dimensionless convective temperature gradient as a function of the pressure throughout the entire convective zone. The results correspond to the 0.6-$M_\odot$ DB WD model at T_{eff} of 26 400 K and $Z = 10^{-3}$ according to the CGM and CM models, and the ML2 and ML3 versions of the MLT. The higher convective fluxes characterizing the CGM model yield slightly deeper convective zones than those given by CM.

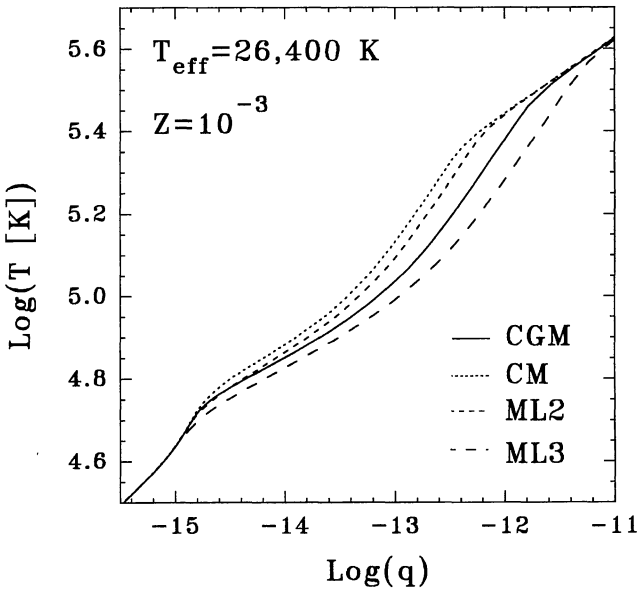

Figure 9. The temperature versus the logarithm of the mass fraction in the convective envelope of a 0.6-$M_\odot$ DB WD model at $T_{\rm eff}$ of 26 400 K and $Z=10^{-3}$ according to the CGM and CM models, and the ML2 and ML3 versions of the MLT. The peak in $\nabla_{\rm conv}$ corresponds to $\log q \approx -14.8$. Note that at these temperatures the profile does not show any peak, and the thermal profile is determined by the behaviour of $\nabla_{\rm conv}$ in deeper layers where convection is more efficient.

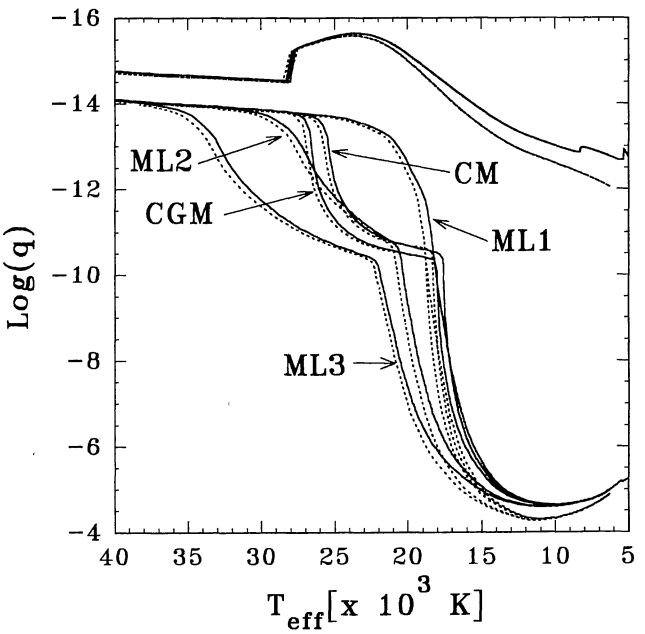

Figure 10. The size of the outer convective zone versus $T_{\rm eff}$ for a 0.4-$M_\odot$ DB WD in different theories of convection as a function of $T_{\rm eff}$. Solid and short-dashed lines stand for the cases of $Z=10^{-3}$ and 0.0, respectively. The top of the convective zone almost coincides with the photosphere and depends only upon metallicity.

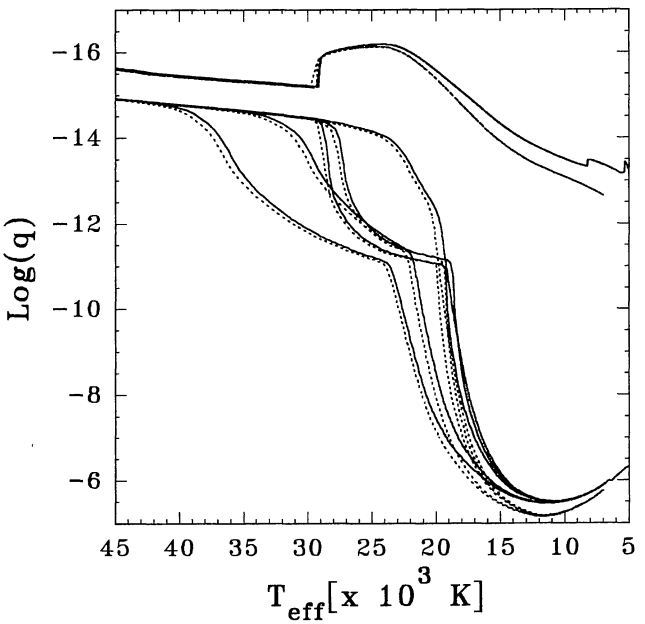

Figure 11. Same as Fig. 10, but for a 0.6-$M_\odot$ DB WD.

treatment of convection. For cool objects, the thermal profile is approximately adiabatic, and the depth reached by the OCZ is limited by the low conductive opacity of the degenerate interior. As the object cools down, deep layers become degenerate, forcing the bottom of the OCZ to retreat outwards. Lower metallicities render the helium plasma more transparent, thus providing a deeper OCZ. This is simply because one needs to get deeper to reach the same temperature compared to the case of higher values of Z. It is worth mentioning that the top of the OCZ depends upon the value of Z but not upon the convection treatment. At $T_{\rm eff} \approx 28\,000$ K, the top of the OCZ undergoes a sharp jump. Such a jump may render suspicious the way one measures z in the case of the FSTs. However, fortunately, in radial coordinates, it represents a small jump that does not affect z significantly. This jump is due to the employment of the Saumon et al. (1995) EOS, which, at the conditions attained at the jump, has a rather poor thermodynamic consistency (see Saumon et al. 1995 for more details).

For the other models, the evolution of the OCZ is given in Figs 11–13. The general trend is qualitatively similar, except for the well-known fact that the more massive the WD, the thinner is the OCZ. For the sake of comparison, we show in Fig. 14 the evolution of the size of the OCZ for models of $M/M_\odot = 0.6$, 0.8 and 1.0 in the CGM. Also, it is important to remark that if $\log q_{\rm He} \geq -6$, the size of the OCZ is insensitive to variations in such a quantity.

Fortunately, as it is well known (see, e.g., Winget et al. 1983 and Tassoul et al. 1990), there exists a way of predicting the blue edge of the instability strip for WD objects without having to perform computations of the periods for non-radial pulsations: the temperature of the theoretical blue edge may be estimated by calculating the $T_{\rm eff}$ at which the thermal time-scale $\tau_{\rm TH}$ defined as

$$\tau_{\rm TH} = \int_0^{q_{\rm bc}} \frac{C_{\rm V} T}{L} M_* \, {\rm d}q \qquad (11)$$

becomes equal to 100 s, which corresponds to the shortest observable g-mode periods. In equation (11), $C_{\rm V}$ is the

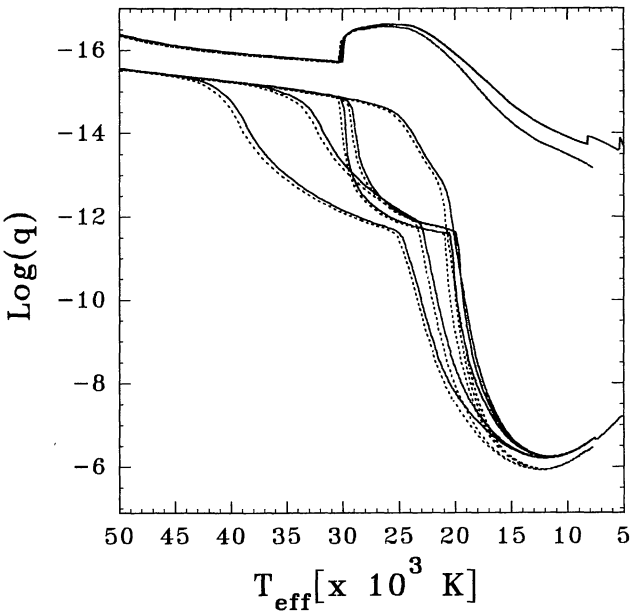

Figure 12. Same as Fig. 10, but for a 0.8-$M_\odot$ DB WD.

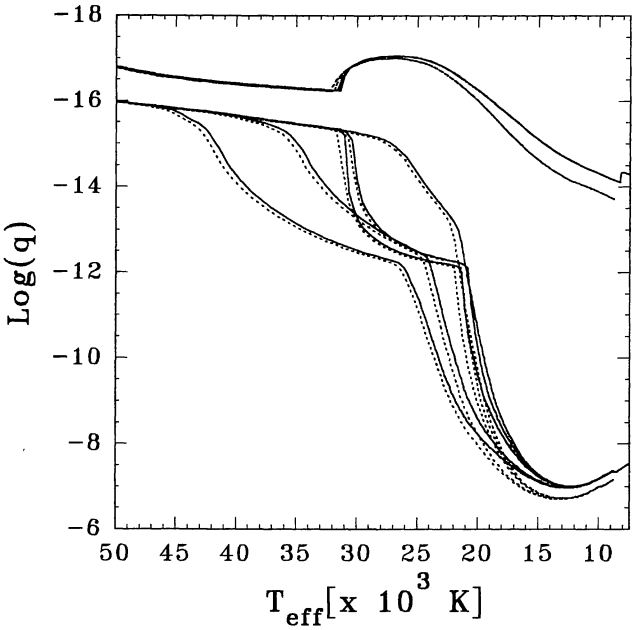

Figure 13. Same as Fig. 10, but for a 1.0-$M_\odot$ DB WD.

specific heat at constant volume, and the subscript 'bc' corresponds to the bottom of the OCZ.

In Fig. 15 we show the $T_{\rm eff}$ of the theoretical blue edge of the DB instability strip for different masses, together with the values corresponding to the observations of Provencal et al. (1996) for the WD GD 358, which is the hottest known member belonging to the DBV class. In this work, we found that the predictions of ML2 and CM are similar, in contrast to the results given in Althaus & Benvenuto (1996). These discrepancies are largely due to differences in the treatment of the EOS for low-density layers. Note that the lower the metallicity, the higher is the $T_{\rm eff}$ of the blue edge. It is important to note that the self-consistent CGM model predicts hotter blue edges than CM, which is in better agreement with observations. Finally, for the sake of completeness, in Fig. 16 we show the theoretical blue edge for the cases of CGM, CM, ML1 and ML3. In Table 1 we give the values of the blue edge for models with $\log q_{\rm He} = -2$ for the different masses, metallicities and con-

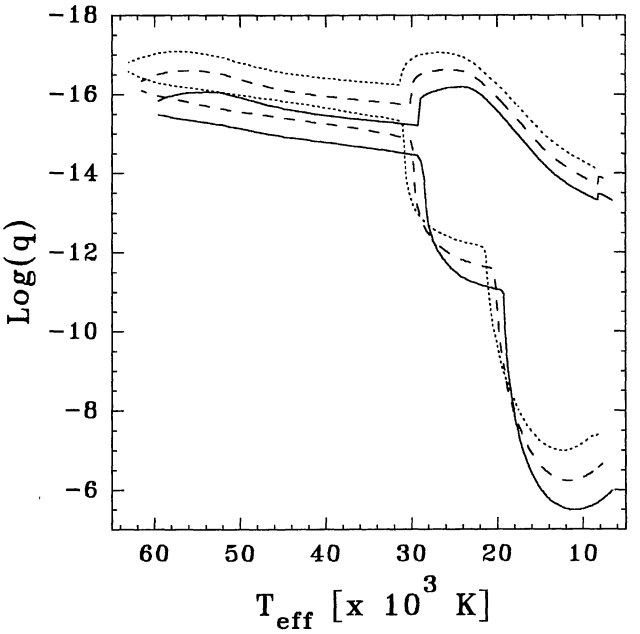

Figure 14. The size of the outer convective zone versus $T_{\rm eff}$ for DB WD models of $M/M_\odot = 0.6$ (solid lines), 0.8 (medium-dashed lines) and 1.0 (short-dashed lines) according to the CGM model.

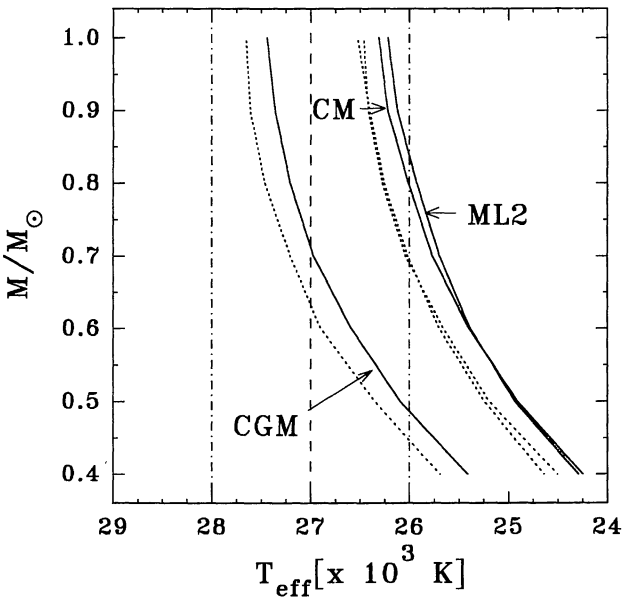

Figure 15. The dependence of theoretical blue edge temperature on the stellar mass for the CGM and CM, and for the ML2. Solid and short-dashed lines stand for the cases of $Z = 10^{-3}$ and 0.0, respectively. We also show the Provencal et al.'s (1996) determination of the DBV GD 358's $T_{\rm eff}$ (27 000 $\pm$ 1000 K). Notice that the agreement with observations is much better in the CGM model than in CM.

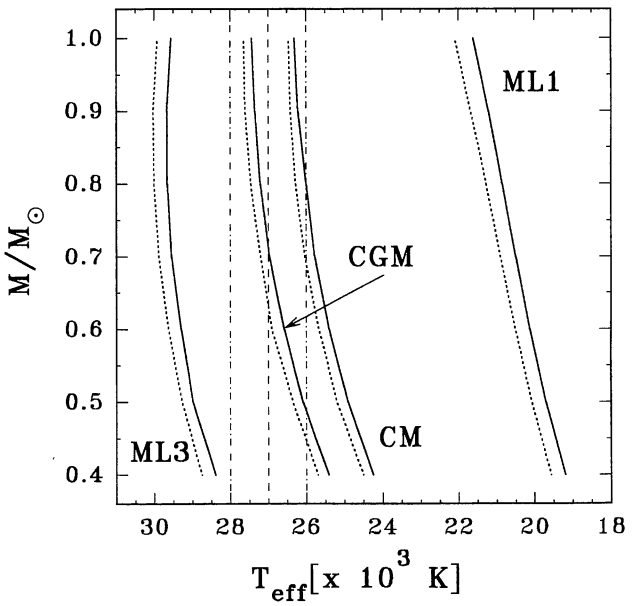

Figure 16. Same as in Fig. 15, but for CGM and CM, and for ML1 and ML3 versions of the MLT.

vection theories we employed. It is important to stress that the blue edge is fairly insensitive to changes in the value of $\log q_{\rm He}$, a fact advanced by Bradley & Winget (1994) based on pulsational studies.

5 DISCUSSION AND CONCLUSIONS

In this paper we compute a set of white dwarf (WD) models with helium-dominated outer layers (DB). The models have masses of $M/\mathrm{M}_{\odot}=0.4$, 0.5, 0.6, 0.7, 0.8, 0.9 and 1.0, helium layer thickness of $\log q_{\rm He}=-2$, -4 and -6, and metallicities of $Z=10^{-3}$ and 0.0. Each evolutionary track was followed from the hot WD stage down to $\log L/\mathrm{L}_{\odot}\lesssim -5$.

The computations were carried out with a full stellar evolution code in which we include a detailed and updated treatment of the equation of state, neutrino emission, radiative and conductive opacities, crystallization and convection. With regard to convection, we employ the two versions presently available of the so-called full spectrum turbulence theory (FST) presented by Canuto & Mazzitelli (1991, 1992) (CM) and Canuto, Goldman & Mazzitelli (1996) (CGM). We also considered the standard treatment of the mixing-length theory (MLT) in the versions currently employed in the study of WDs.

The calculations represent an improvement in the general treatment of the WD evolution, particularly with regard to convection. It is well known that for this kind of object convection is present only in an extremely narrow outer layer which is unable to modify appreciably the age, neutrino emission, etc., so that these quantities are practically independent of the treatment of convection.

However, this is *not* the case with pulsational properties, particularly with the determination of the position of the instability strips. The evolution of the shape of the OCZ is strongly dependent upon the convection theory. For example, the OCZ predicted by CM and CGM is very different from that given by the various versions of the MLT, irrespective of the choice for the parameters of the latter.

Table 1. Theoretical blue edge effective temperatures for our DB WD models.

Theory of Convection	Mass $(M/M_{\odot})$	$T_{\rm eff}$ (K) $(Z=10^{-3})$	$T_{\rm eff}$ (K) $(Z=0.0)$
CGM	0.40	25,410	25,692
CM	"	24,250	24,508
ML1	"	19,190	19,570
ML2	"	24,290	24,640
ML3	"	28,380	28,750
CGM	0.50	26,090	26,349
CM	"	24,910	25,194
ML1	"	19,700	20,070
ML2	"	24,930	25,240
ML3	"	28,990	29,280
CGM	0.60	26,590	26,902
CM	"	25,400	25,659
ML1	"	20,130	20,510
ML2	"	25,390	25,700
ML3	"	29,300	29,630
CGM	0.70	26,970	27,206
CM	"	25,770	26,039
ML1	"	20,510	20,900
ML2	"	25,700	26,020
ML3	"	29,560	29,890
CGM	0.80	27,210	27,465
CM	"	26,010	26,275
ML1	"	20,860	21,280
ML2	"	25,930	26,250
ML3	"	29,670	30,014
CGM	0.90	27,360	27,611
CM	"	26,220	26,418
ML1	"	21,220	21,680
ML2	"	26,120	26,400
ML3	"	29,670	30,040
CGM	1.00	27,440	27,653
CM	"	26,310	26,466
ML1	"	21,620	22,110
ML2	"	26,220	26,520
ML3	"	29,570	29,910

Comparing CM and CGM results, small differences in the structure of the OCZ appear. This fact is reminiscent of the findings of CGM in the application to the Sun and Population II objects. However, these differences turn out to be appreciable in the position of the blue edge of the instability strip. This becomes relevant at the moment of choosing the theory that produces the best fit with observations.

As is well known, GD 358 observationally defines the blue edge of the DB instability strip. Because of this fact, this star has captured the attention of various studies for quite some time. Thejll et al. (1991) reported a determination of $T_{\rm eff}=24\,000\pm1000$ K, whereas the most recent determination (Provencal et al. 1996) gives $T_{\rm eff}=27\,000\pm1000$ K, which represents an important increase in the accepted $T_{\rm eff}$ for this star.

In a previous paper (Althaus & Benvenuto 1996), we have shown that CM predicts a blue edge $T_{\rm eff}$ in good agreement with the observations of Thejll et al. (1991). However, this is not the case with the newer measurements of Provencal et al. (1996). However, in the frame of the CGM model, the situation is just the opposite: theoretical results match Provencal et al. observations but not Thejll et al. ones. Thus, if we accept Provencal et al. value for the $T_{\rm eff}$ of GD 358, we must conclude that, at least in the realm of DB WDs, CGM clearly works better than its predecessor CM (see also Althaus & Benvenuto 1997b). This is, in our opinion, the main finding of the present work. The agreement between theory and observation is quite natural, strongly suggesting that the description provided by the models based on the FST approach to describe convection is definitely better than that provided by the MLT in its different guises. We think that these results would justify an effort in computing pulsational modes of WD models constructed with the assumptions about convection we have made in the present work.

In working on this topic extensive tabulations of the evolution of DB WDs have been constructed. These tabulations are not included here, but are available upon request to the authors at their e-mail address.

ACKNOWLEDGMENTS

We thank F. Rogers and I. Mazzitelli for sending us their opacity and equation of state data, respectively. We also thank V. Canuto for comments on the initial version of this paper. This work has been partially supported by the Comisión de Investigaciones Científicas de la Provincia de Buenos Aires, the Consejo Nacional de Investigaciones Científicas y Técnicas under the PROgrama de FOtometría y Estructura Galáctica (PROFOEG) and the Universidad Nacional de La Plata (Argentina).

REFERENCES

Althaus L. G., Benvenuto O. G., 1996, MNRAS, 278, 981
Althaus L. G., Benvenuto O. G., 1997a, ApJ, 477, 313 (AB97)
Althaus L. G., Benvenuto O. G., 1997b, MNRAS, in press
Benvenuto O. G., Althaus L. G., 1995, Ap&SS, 234, 11
Bergeron P., Saffer R A., Liebert J., 1992, ApJ, 394, 228
Böhm K.-H., Cassinelli J. P., 1971, A&A, 12, 21
Böhm-Vitense E., 1958, Z. Astrophys., 46, 108
Bradley P. A., 1996, ApJ, 468, 350
Bradley P. A., Winget D. E., 1994, ApJ, 421, 236
Bragaglia A., Renzini A., Bergeron P., 1995, ApJ, 443, 735
Canuto V. M., 1996, ApJ, 467, 385
Canuto V. M., Mazzitelli I., 1991, ApJ, 370, 295 (CM)
Canuto V. M., Mazzitelli I., 1992, ApJ, 389, 724 (CM)
Canuto V. M., Goldman I., Mazzitelli I., 1996, ApJ, 473, 550 (CGM)
Chandrasekhar S., 1939, An Introduction to the Study of Stellar Structure. Univ. Chicago Press, Chicago
Cox A. N., Stewart J., 1970, ApJS, 19, 261
D'Antona F., Mazzitelli I., 1989, ApJ, 347, 934
D'Antona F., Mazzitelli I., 1990, ARA&A, 28, 139
D'Antona F., Mazzitelli I., 1994, ApJS, 90, 467
D'Antona F., Mazzitelli I., Gratton R. G., 1992, A&A, 257, 539
Hubbard W. B., Lampe M., 1969, ApJS, 18, 297
Iben I., Tutukov A., 1984, ApJ, 282, 615
Kippenhahn R., Weigert A., Hofmeister E., 1967, in Alder B., Fernbach S., Rottenberg M., eds, Methods in Computational Physics, 7. Academic Press, New York, p. 129
Koester D., Chanmugam G., 1990, Rep. Prog. Phys., 53, 837
Koester D., Schönberner D., 1986, A&A, 154, 125
Lamb D. Q., Van Horn H. M., 1975, ApJ, 200, 306
Ludwig H. G., Jordan S., Steffen M., 1994, A&A, 284, 105
Magni G., Mazzitelli I., 1979, A&A, 72, 134
Mazzitelli I., D'Antona F., 1991, in Vauclair G., Sion E. M., eds, Seventh European Workshop on White Dwarfs (NATO ASI Series). Kluwer, Dordrecht, p. 305
Mestel L., 1952, MNRAS, 112, 583
Mihalas D., 1970, Stellar Atmospheres. Freeman, San Francisco
Oswalt T. D., Smith J. A., Wood M. A., Hintzen P., 1996, Nat, 382, 692
Paternó L., Ventura R., Canuto V. M., Mazzitelli I., 1993, ApJ, 402, 733
Provencal J. L., Shipman H. L., Thejll P., Vennes S., Bradley P. A., 1996, ApJ, 466, 1011
Renzini A. et al., 1996, ApJ, 465, L23
Richer B. H. et al., 1995, ApJ, 451, L17
Saumon D., Chabrier G., Van Horn H. M., 1995, ApJS, 99, 713
Shapiro S. L., Teukolsky S. A., 1983, Black holes, White Dwarfs and Neutron Stars: The Physics of Compact Objects. Wiley-Interscience, New York
Stothers R. S., Chin C.-W., 1995, ApJ, 440, 297
Tassoul M., Fontaine G., Winget D. E., 1990, ApJS, 72, 335
Thejll P., Vennes S., Shipman H. L., 1991, ApJ, 370, 355
Von Hippel T., Gilmore G., Jones D. H. P., 1995, MNRAS, 273, L39
Van Horn H. M., 1968, ApJ, 151, 227
Wesemael F., Bergeron P., Fontaine G., Lamontagne R., 1991, in Vauclair G., Sion E. M., eds, Seventh European Workshop on White Dwarfs (NATO ASI Series). Kluwer, Dordrecht, p. 159
Winget D. E., Van Horn H. M., Tassoul M., Hansen C. J., Fontaine G., Carroll B. W., 1982, ApJ, 252, L65
Winget D. E., Van Horn H. M., Tassoul M., Hansen C. J., Fontaine G., 1983, ApJ, 268, L33
Wood M. A., 1992, ApJ, 386, 539